A dynamic control strategy to produce riboflavin with lignocellulose hydrolysate in the thermophile *Geobacillus thermoglucosidasius*

Junyang Wang
Institute of Microbiology
Zilong Li
Institute of Microbiology
Weishan Wang
Institute of Microbiology https://orcid.org/0000-0001-7827-2696
Shen Pang
State Key Laboratory of Microbial Resources, Institutue of Microbiology, Chinese Academy of Scienceses
Fengxian Qi
State Key Laboratory of Microbial Resources, Institutue of Microbiology, Chinese Academy of Scienceses
Yongpeng Yao
State Key Laboratory of Microbial Resources, Institutue of Microbiology, Chinese Academy of Scienceses
Fang Yuan
Hebei Shengxue Dacheng Pharmaceutical Co. Ltd.
Huizhuan Wang
Hebei Shengxue Dacheng Pharmaceutical Co. Ltd.
Zhen Xu
Hebei Shengxue Dacheng Pharmaceutical Co. Ltd.
Guohui Pan
State Key Laboratory of Microbial Resources, Institutue of Microbiology, Chinese Academy of Sciences
Yihua Chen
State Key Laboratory of Microbial Resources & CAS Key Laboratory of Microbial Physiological and Metabolic Engineering, Institute of Microbiology, Chinese Academy of Sciences https://orcid.org/0000-0001-9362-512X
Keqiang Fan (fankq@im.ac.cn)
State Key Laboratory of Microbial Resources, Institutue of Microbiology, Chinese Academy of Scienceses https://orcid.org/0000-0003-2420-1889

Article

Keywords: metabolic engineering, biosynthesis, GCR-based dynamic control (GCR-DC) strategy

Posted Date: January 27th, 2021

DOI: https://doi.org/10.21203/rs.3.rs-151219/v1

Abstract

The efficient utilization of both glucose and xylose, the two most abundant sugars in biomass hydrolysates, is one of the main objectives of biofermentation with lignocellulosic materials. The utilization of xylose is commonly inhibited by glucose, which is known as glucose catabolite repression (GCR). Here we report a GCR-based dynamic control (GCR-DC) strategy aiming at a better co-utilization of glucose and xylose, by decoupling the cell growth and biosynthesis of riboflavin as a product. Using the thermophilic strain *Geobacillus thermoglucosidasius* DSM2542 as a host, we constructed extra riboflavin biosynthetic pathways that were activated by xylose but not glucose. The engineered strains showed a two-stage fermentation process. In the first stage, glucose was preferentially used for cell growth and no production of riboflavin was observed, while in the second stage where glucose was nearly depleted, xylose was effectively utilized for riboflavin biosynthesis. Using the corn cob hydrolysate as a carbon source, the optimized riboflavin yields of strains DSM2542-DCall-MSS (full pathway dynamic control strategy) and DSM2542-DCrib (single module dynamic control strategy) were 5.26 and 2.26 folds higher than that of the control strain DSM2542 Rib-Gtg constitutively producing riboflavin, respectively. This GCR-DC strategy should also be applicable to the construction of cell factories that can efficiently use natural carbon sources with multiple sugar components for the production of high-value chemicals in future.

Introduction

The biofermentation industry has now become an important alternative of petrochemical industry in terms of producing various valuable products, including biofuels, solvents and fine chemicals. To date, many biofermentation processes rely on glucose-based substrates, such as starch and molasses. Extending the utilization ability towards other substrates, like the natural carbon source lignocellulose[1–4] that contains glucose and xylose as the two most abundant sugars[4–7], would be attractive for biofermentation in the aspects of cost control and the production of valuable glucose/xylose derived products.

Riboflavin (vitamin B_2) is the precursor of FMN and FAD, which are indispensable for normal cellular activities of both prokaryotic and eukaryotic organisms[8–10]. As an essential vitamin, riboflavin has been widely used in many fields, such as pharmaceuticals, food additives, cosmetics, and animal feed[10–12]. Riboflavin is biosynthesized from two pentose derived precursors, ribulose 5-phosphate (Ru5P) and GTP[10,12]. The Gram-positive bacterium *Bacillus subtilis* is one of the widely used industrial host for the production of riboflavin, which mainly uses glucose as a carbon source[9,13–17]. Therefore, the production costs should be reduced if the cheap lignocellulosic hydrolysates can be used to replace glucose. In addition, the mesophilic fermentation of *B. subtilis* is often plagued by contaminated bacteria and the large amount of heat generated during fermentation[18,19]. This issue might be overcame by using thermophilic bacteria that can be fermented at high temperature[19–21].

The thermophile *Geobacillus thermoglucosidasius* DSM 2542 (also known as *Parageobacillus thermoglucosidasius* DSM 2542) is a promising chassis organism for biofermentation, due to its prominent properties including the rapid growth under thermophilic fermentation conditions, the capability of utilizing a wide range of carbon sources, and the genetic amenability[19,20]. *G. thermoglucosidasius* has been successfully used to produce ethanol[19,22]. Significantly, *G. thermoglucosidasius* can efficiently utilize both glucose and xylose, the two main components of lignocellulose hydrolysate, as carbon sources[18,19]. Xylose is firstly taken into cells by its transporters, and converted to xylulose by xylose isomerase (XylA)[23,24]. Then, xylulose is converted to 5-phosphate xylulose (Xu5P) by xylose kinase (XylB), which is then transformed into Ru5P, an intermediate of the pentose phosphate pathway[23,24]. As Ru5P is a precursor of riboflavin, xylose would be an appropriate carbon source for the biosynthesis of riboflavin. These features collectively make *G. thermoglucosidasius* an attractive platform for the production of riboflavin.

Xylose uptake and catabolism are often subject to glucose catabolite repression (GCR, also generally known as carbon catabolite repression)[4,25–27]. In bacteria, the xylose-utilizing genes are commonly repressed by the presence of glucose[28–30]. Thus, the utilization of xylose only starts when glucose is exhausted. One way for the co-utilization of glucose and xylose is to remove GCR, which has been demonstrated in many studies[4,27,31–33]. However, the existence of GCR has its own metabolic and evolutionary advantages, such as the ability to selectively utilize carbon sources favorable for cell growth[25]. To take the advantage of that, an alternative strategy would be to utilize glucose and xylose in separate stages for different purposes, e.g. glucose for cell growth and xylose for the biosynthesis of desired product.

Here we designed a GCR based-dynamic control (GCR-DC) strategy and applied it to the engineering of *G. thermoglucosidasius* DSM 2542 for the production of riboflavin. An extra metabolic pathway from xylose to riboflavin was constructed using the xylose-inducible but glucose-insensitive promoters in DSM 2542. This resulted in the decoupling of cell growth and the biosynthesis of riboflavin. The engineered strains preferentially utilized glucose for cell growth due to the presence of GCR, and then switched to the use of xylose for the effective production of riboflavin. The engineered strains produced significantly higher amount of riboflavin in comparison to the control strain constitutively producing riboflavin using mixed glucose and xylose or lignocellulose hydrolysate as carbon sources. This powerful GCR-DC strategy should also be applicable to construct cell factories to produce other valuable products using natural carbon sources like lignocellulose hydrolysate.

Results

Engineering of *G. thermoglucosidasius* DSM 2542 for riboflavin production. In a previous study, we identified the riboflavin biosynthetic gene cluster (*rib* cluster) in *G. thermoglucosidasius* DSM 2542, and overexpressed the *rib* cluster (under the control of the constitutive *ldh* promoter) in *G. thermoglucosidasius* DSM 2542 to obtain DSM 2542 Rib-Gtg[18,21]. As expected, the engineered strain

DSM 2542 Rib-Gtg produced riboflavin at a yield of 58.4 ± 1.6 mg/L using 2% (w/v) xylose as a carbon source, while the wild type strain DSM 2542 did not produce detectable riboflavin (Fig. 2a). This showed that *G. thermoglucosidasius* could be used as a host to produce riboflavin with xylose as a carbon source.

We then evaluated the cell growth and riboflavin production of DSM2542 Rib-Gtg using mixed glucose and xylose, or one of them as carbon sources (Fig. 2b-d). When DSM2542 Rib-Gtg was cultivated using mixed glucose and xylose, GCR phenomenon was observed shown by that the utilization of xylose only occurred after glucose being exhausted (Fig. 2b). The substrate consuming rate and the growth rate of DSM2542 Rib-Gtg were much higher with glucose than those with xylose as a carbon source (Fig. 2c and Supplementary Fig. 1). And the maximum cell density of DSM2542 Rib-Gtg was also higher with glucose than that with xylose (Fig. 2c). On the contrary, the riboflavin production of DSM2542 Rib-Gtg with glucose was significantly lower than that with xylose especially at time points beyond 10 h (Fig. 2d). These results showed that glucose is conducive to cell growth of *G. thermoglucosidasius*, while xylose is more beneficial for the riboflavin production.

Design of a GCR-DC strategy for riboflavin production. Based on the difference between the metabolic features of glucose and xylose, we proposed that decoupling of the cell growth and riboflavin biosynthesis according to their different propensities for carbon source utilization would benefit the riboflavin production of *G. thermoglucosidasius*. We therefore designed a GCR-DC strategy for riboflavin production in *G. thermoglucosidasius* DSM 2542 as depicted in Fig. 1. An extra riboflavin biosynthetic pathway, which was under the control of xylose-inducible and glucose-insensitive promoters, was introduced into the strain DSM 2542, while the native riboflavin biosynthetic gene cluster was retained to supply necessary amount of riboflavin for normal cellular activities. As a result, the fermentation process of the designed strain using mixed glucose and xylose is divided into two stages. In the first stage, glucose is preferentially utilized for cell growth, and the riboflavin biosynthesis is not induced. When glucose is almost used up, the fermentation process would switch to the second stage autonomously, in which the xylose-inducible and glucose-insensitive promoters could sense the dynamic changes of carbon sources and turn on the reconstituted biosynthetic pathway for riboflavin production using xylose.

Discovery and characterization of xylose-inducible and glucose-insensitive promoters from *G. thermoglucosidasius* DSM 2542. Since there was no applicable xylose-inducible and glucose-insensitive promoters in *Geobacillus*, we set to discover those promoters from *G. thermoglucosidasius* DSM 2542. We performed whole genome transcriptional analysis of DSM 2542 with or without xylose to identify xylose-inducible promoters. As shown in Supplementary Fig. 2a, DSM 2542 was cultured in USYE medium with or without 1% xylose, and harvested in the exponential (4 h), transitional (6 h), and stationary phases (8 h). The genes were considered to be activated by xylose when their transcriptional levels were two-fold higher in xylose-containing culture than those in xylose-free culture. A hierarchical clustering analysis resulted in a total of 71 xylose-activated genes (Supplementary Fig. 2b-c and Supplementary Table 1, 2). In bacterial genomes, several genes are often organized into an operon and co-transcribed under the control of a single promoter[34]. Operon analysis revealed that 59 out of the 71

genes were from 27 predicted operons, and the remaining 12 genes were transcribed individually (Supplementary Table 3). Hence, there were totally 39 putative xylose-inducible promoters. Among them, 20 were selected to cover a broad range of transcriptional levels (Supplementary Fig. 3). The 500-bp sequences upstream of the coding sequence of the first gene within each operon were used as the putative xylose-inducible promoters for further evaluation (Supplementary Table 4).

The strengths of the 20 putative promoters were evaluated by a green fluorescent protein (GFP) reporter system in DSM 2542 (Fig. 3a). The fluorescence assay of the 20 strains DSM2542-n (n referred to the promoter being used for the control of GFP expression) revealed that 1% xylose could increase the expression levels of GFP in all strains, suggesting that all the 20 promoters could be activated by xylose (Fig. 3b and Supplementary Fig. 4a). The strengths of the 20 promoters reflected by the GFP fluorescence intensities varied in a large range, and the results were overall consistent with the transcriptional levels of their corresponding genes (Supplementary Fig. 3).

To select the promoters that are activated by xylose but not glucose (glucose-insensitive), the 20 promoters were further trimmed to nine (labelled by asterisks in Fig. 3b) by removing 11 of them that still showed significant expression levels when xylose was not added (Fig. 3b). The nine promoters were further evaluated by cultivating their corresponding strains in the medium with 1% glucose, and all the strains emitted little fluorescence (Supplementary Fig. 4b), showing that the nine promoters are glucose-insensitive.

The dynamic regulation profiles were evaluated in detail using promoter P_{11585}, the native promoter of the xylose-utilizing genes *xylA* and *xylB*. The strain DSM2542-RS11585 (harboring the GFP reporter system driven by P_{11585}) was cultivated in USYE medium containing 1% glucose + 1% xylose. At the early stage (2 − 6 h), the strain consumed glucose preferentially and no fluorescence was observed (Fig. 3c). After glucose was used up, xylose started to be consumed with the GFP fluorescence intensity increasing gradually (6 − 14 h). The results suggested that, as anticipated, the promoter P_{11585} could be efficiently activated by xylose but not glucose. Further GFP fluorescence assays of DSM2542-RS11585 revealed a dose-dependent activation of the promoter P_{11585} by different concentrations of xylose (0 − 1.0%) (Fig. 3d). Taken together, we identified nine xylose-inducible but glucose-insensitive promoters that could be used in the dynamic control strategy for decoupling cell growth and riboflavin production.

Production of riboflavin in *G. thermoglucosidasius* using the GCR-DC strategy. We next used the promoter P_{11585} to evaluate the GCR-DC strategy for riboflavin production. The plasmid harboring the *rib* cluster (under the control of P_{11585}) from DSM 2542 was constructed, and reintroduced into DSM 2542 to obtain the strain DSM2542-DCrib (Fig. 4a). DSM2542-DCrib was first cultured in USYE medium containing 2% xylose or 2% glucose, respectively. The production of riboflavin was only observed in the former medium (121.0 ± 2.4 mg/L) but not in the latter one (Fig. 4a). Then, DSM2542-DCrib was fermented in USYE medium with mixed 1% glucose and 1% xylose. At the first stage (2 − 6 h), glucose was consumed preferentially, and the cell density increased to OD_{600} 4.5 with no riboflavin accumulated; at the second stage (after 6 h) where glucose was nearly depleted, xylose began to be consumed with riboflavin being

accumulated gradually and reaching a yield of 59.4 ± 1.3 mg/L at 24 h (Fig. 4b). These results showed that the cell growth and riboflavin production was indeed decoupled in DSM2542-DCrib as expected.

Next, we aimed to control the whole pathway from xylose to riboflavin dynamically using this strategy. The whole metabolic pathway could be divided into four modules (Fig. 1): (I) xylose utilization module contains the aforementioned *xylA* and *xylB* genes [29,32]. Their native promoter, P_{11585}, has been identified as a strong xylose-inducible promoter in this study. (II) phosphoribosyl pyrophosphate (PRPP) biosynthesis module converts Xu5P to PRPP, in which the gene *prs* encoding the phosphoribosylpyrophosphate synthetase is regulated by feedback inhibition of downstream metabolites, such as ADP and GDP[35,36]. (III) purine biosynthesis module is responsible for the conversion of PRPP to GTP[17,37]. This module contains the genes of the *pur* operon and other downstream genes. Particularly, the 12 genes from the *pur* operon are organized as a cluster, whose transcription is strictly regulated by the repressor PurR[37–41]. (IV) riboflavin biosynthesis module (the *rib* cluster) that combines Ru5P and GTP into riboflavin is regulated by the downstream product FMN[8,36,42]. As module I is already under the control of the native xylose-inducible promoter P_{11585}, engineering is required for the remaining three modules to get rid of the original regulations and make them xylose-inducible (Fig. 1). Three xylose-inducible promoters with varied strengths (the strong promoter P_{11585} (S), a medium strength promoter P_{16610} (M), and a weak promoter P_{03225} (W)) were used to activate each of the three modules, and a total of 27 combinations were tested to find out the best combination for riboflavin production (Fig. 3b and 5a). The plasmids harboring the three modules controlled by different combinations of promoters were constructed by yeast-based transformation-associated recombination method[43,44], and then transferred to DSM 2542 to generate 27 engineered strains, in which the extra metabolic pathway from xylose to riboflavin was mainly controlled by xylose-inducible promoters.

The riboflavin productions of the 27 engineered strains were measured in USYE medium with 2% xylose at 24 h. Among them, the strain DSM2542-DCall-MSS showed the highest riboflavin titer (273.0 ± 3.2 mg/L). In DSM2542-DCall-MSS, module II was driven by the medium strength promoter P_{16610}, and both modules III and IV were controlled by the strong promoter P_{11585} (Fig. 5b and Supplementary Table 5). Due to its highest production, this strain was used for further studies.

Determination of the optimal xylose/glucose ratio for DSM2542-DCall-MSS to produce riboflavin. The switching time from cell growth stage to riboflavin production stage in DSM2542-DCall-MSS is dictated by the ratio of xylose and glucose. If the optimal xylose/glucose ratio for the production of riboflavin in DSM2542-DCall-MSS is close to the ratio of the two sugars in certain natural carbon sources, this strain presumably can directly use those natural carbon sources for biofermentation. To identify the optimal ratio of xylose/glucose, DSM2542-DCall-MSS was fermented in USYE medium containing mixed glucose and xylose at different ratios. The total sugar concentration was set to 2% (w/v), in which the percentage of xylose ranged from 20–78%. The highest yield of riboflavin reached 317.0 ± 6.1 mg/L when the percentage of xylose was 67% (xylose/glucose: 2:1) (Fig. 6a). When the proportion of xylose was at an

optimal range from 50–80% (xylose/glucose: 1:1 to 4:1), the riboflavin yields were all above 250 mg/L (Fig. 6a).

Production of riboflavin using the lignocellulosic carbon source corn cob hydrolysate. For many lignocellulosic materials, the xylose/glucose ratios are within the aforementioned optimal range (1:1 to 4:1) for DSM2542-DCall-MSS. For example, the corn cob hydrolysate used in this study had a sugar contents of 52% xylose, 18% glucose, 15% L-arabinose, and 15% galactose as determined by HPLC, which showed the xylose/glucose ratio is around 3:1. This suggested that DSM2542-DCall-MSS could use corn cob hydrolysate as a carbon source to produce riboflavin. The aforementioned strains DSM2542-DCrib (the *rib* cluster controlled by the xylose-inducible promoter P_{11585}) and DSM2542 Rib-Gtg (the *rib* cluster controlled by the constitutive promoter *pldh*) were used as controls. The three strains were fermented in USYE medium containing 0.5% or 1.0% (w/v) corn cob hydrolysate. The riboflavin yields of all the three strains with 0.5% corn cob hydrolysate were higher than those with 1% corn cob hydrolysate, which might be due to the presence of furfural and other substances in the corn cob hydrolysate that are adverse to cell growth[45]. With 0.5% corn cob hydrolysate, the riboflavin titer of DSM2542-DCall-MSS reached 121.0 ± 8.0 mg/L, which were 5.26 and 2.33 times higher than those of DSM2542 Rib-Gtg and DSM2542-DCrib, respectively (Fig. 6b and Supplementary Table 6). And as anticipated, the dynamic control of riboflavin production was achieved by decoupling the riboflavin biosynthesis from cell growth (Fig. 6c). These results supported that the dynamic control strategy was effective to improve the utilization of lignocellulosic hydrolysates by giving full play to the distinct metabolic advantages of different sugars.

Discussion

The efficient utilization of renewable lignocellulose biomass has always been one of the major goals for biofermentation. As the second abundant sugar in lignocellulose hydrolysate after glucose, xylose makes up 30–40% of lignocellulosic biomass[6,46]. Although many microorganisms can use both sugars, glucose is generally preferred to be utilized due to GCR[25]. To improve the utilization of lignocellulosic hydrolysates, studies have achieved the co-utilization of glucose and xylose by removing GCR through genetic engineering[7,47–52]. However, the existence of GCR endows the host strains unique advantages. Especially, the preference to the utilization of glucose greatly facilitates the cell growth of host strains, which is also true for the thermophile *G. thermoglucosidasius* DSM 2542 in this study (Fig. 2c). Therefore, an alternative strategy to improve the utilization of lignocellulosic hydrolysates is to take advantages of the different metabolic characteristics of glucose and xylose. A previous study reported a two-phase fed-batch strategy for the production of poly(lactate-co-3-hydroxybutyrate) in *Escherichia coli*[53]. In their strategy, glucose was used for cell growth in the initial stage, and xylose was manually added in the second stage for polymer production, which resulted in a higher production of polymer than that of using xylose or glucose alone[53]. This exemplified an efficient way to use glucose and xylose for cell growth and the biosynthesis of desired product, respectively. However, the requirement of manual addition of xylose precludes the application of this strategy to natural carbon sources like lignocellulosic hydrolysates that contain both glucose and xylose.

As an essential vitamin, riboflavin is biosynthesized from Ru5P and GTP, both of which can be derived from xylose[10]. In this study, we first showed that xylose, in comparison to glucose, was a better carbon source for riboflavin production in *G. thermoglucosidasius* DSM 2542, while glucose was more conducive to cell growth. Taking advantages of GCR and the distinct metabolic properties of the two sugars, we used xylose-inducible and glucose-insensitive promoters to reconstruct a riboflavin biosynthetic pathway (from xylose to riboflavin), and as expected, the riboflavin production and cell growth was decoupled in the engineered strain. The application of this GCR-DC strategy led to a significantly higher production of riboflavin in comparison to that of strains constitutively producing riboflavin (Fig. 6). As many high-value chemicals, such as FMN, FAD, inosine, and guanosine, can be derived from pentose phosphate pathway, the GCR-DC strategy should also be applicable for the production of those products.

The 27 engineered DSM2542-DCall strains each controlled by a unique set of promoters, displayed a wide range of riboflavin yields (Fig. 5). Among them, the strain DSM2542-DCall-MSS exhibited highest riboflavin production. This has once again showed that tuning the expression levels of biosynthetic genes is critical to achieve the maximal biosynthetic capacity of a pathway[54–56]. The bunch of newly identified xylose-inducible and glucose-insensitive promoters with a broad range of strengths, provide expedient genetic tools for the further engineering of *G. thermoglucosidasius* DSM 2542.

In this study, *G. thermoglucosidasius* DSM 2542 was used as a platform host for the production of riboflavin, mainly due to its rapid growth and thermophilic fermentation features. Especially, the thermophilic fermentation helped cut down the cost for cooling and significantly reduce the occurrence of contamination during fermentation. Therefore, *G. thermoglucosidasius* DSM 2542 is emerging as an attractive platform for biofermentation. Other strategies, including deletion of the regulatory gene *ccpN*, gene encoding lactic dehydrogenase and certain genes involved in the purine metabolic network[21,57], engineering of the riboswitches of *pur* and *rib* operons[58] and the RBS regions of genes involved in riboflavin biosynthesis[59], and introducing mutations in the transcriptional regulators CcpN and YvrH[16], have also been successful to increase the production of riboflavin. These approaches might be integrated with our GCR-DC strategy to further improve the capacity of this robust host, *G. thermoglucosidasius* DSM 2542, to utilize natural carbon sources for the production of riboflavin and other high-value products in future.

Methods

Strains, media and culture conditions. Bacterial strains used in this study are shown in Supplementary Table 7. *E. coli* strains were grown in lysogeny broth (LB) medium with 12.5 μg/mL kanamycin added when needed. USYE media were used during the genetic manipulation and fermentation of *G. thermoglucosidasius*, respectively, as described previously[19,21]. D-glucose and/or D-xylose were added in USYE medium as declared with the final concentrations of 2% (w/v) glucose, 2% (w/v) xylose, or 1% (w/v) glucose + 1% (w/v) xylose, respectively. The engineered *G. thermoglucosidasius* strains were cultivated in 250 mL shake flask with 50 mL USYE medium containing 40 mM each (final concentrations) of Bis-Tris,

PIPES, and HEPES at pH 7.0 as a seed culture. Then, 0.5 mL seed culture was added to 50 mL USYE medium (Glucose and/or xylose were added as declared) and fermented for designated time at 60°C, 250 rpm.

For yeast culture, the rich medium YPD was used for the routine growth of yeast strain BJ5464-NpgA and its derivatives at 28°C[43,44,60]. UDMS media were used for the selection of plasmids constructed by yeast homologous recombination as previously described[44]. The yeast transformants were grown on the solid UDMS medium for 2 − 4 days.

Construction of plasmids and engineered strains. All plasmids used in this work are listed in Supplementary Table 7. All primers and oligonucleotides are listed in Supplementary Table 8. The genomic DNA was extracted from *G. thermoglucosidasius* DSM 2542 using the Ultraclean® Microbial DNA Isolation kit from Mo Bio Laboratories, Inc. (Cambio Ltd., Cambridge, UK) according to the manufacturer's protocol. Plasmid extractions were performed using NucleoSpin Plasmid EasyPure kit (Macherey-Nagel). PCR screening for transformants were carried out with Taq 2× Master Mix (TsingKe, China).

To characterize the xylose-inducible promoters, the selected 20 putative promoters were amplified from the genome of *G. thermoglucosidasius* DSM 2542 using the primer pairs RS10605-F/R, RS03330-F/R, RS11585-F/R, RS19825-F/R, RS08295-F/R, RS11580-F/R, RS07185-F/R, RS05470-F/R, RS07230-F/R, RS06405-F/R, RS11780-F/R, RS01665-F/R, RS07175-F/R, RS11470-F/R, RS07200-F/R, RS16610-F/R, RS07150-F/R, RS11785-F/R, RS01820-F/R and RS03225-F/R, and assembled with the corresponding plasmid backbone amplified from pUCG18-sfgfp using the primer pairs pUCG18-RS10605-F/R, pUCG18-RS03330-F/R, pUCG18-RS11585-F/R, pUCG18-RS19825-F/R, pUCG18-RS08295-F/R, pUCG18-RS11580-F/R, pUCG18-RS07185-F/R, pUCG18-RS05470-F/R, pUCG18-RS07230-F/R, pUCG18-RS06405-F/R, pUCG18-RS11780-F/R, pUCG18-RS01665-F/R, pUCG18-RS07175-F/R, pUCG18-RS11470-F/R, pUCG18-RS07200-F/R, pUCG18-RS16610-F/R, pUCG18-RS07150-F/R, pUCG18-RS11785-F/R, pUCG18-RS01820-F/R and pUCG18-RS03225-F/R by Gibson assembly[61], respectively, generating 20 plasmids pUCG18-n-sfgfp (n indicates the name of the selected 20 promoters, see Supplementary Table 7). The 20 plasmids were transformed into *G. thermoglucosidasius* DSM 2542 to generate the corresponding 20 engineered strains DSM2542-n (n indicates the name of the selected 20 promoters, see Supplementary Table 7).

To construct the plasmid pUCG18-RS11585-Gtribo (Supplementary Table 7), the *rib* cluster was amplified from the genome of DSM 2542 using the primer pair 11585Gtrib-F/R and assembled with the plasmid backbone amplified from pUCG18-RS11585-sfgfp using the primer pair 11585Gtrib-GJ-F/R by Gibson assembly[61]. The plasmid pUCG18-RS11585-Gtribo was transformed into DSM 2542 by electroporation to generate the strain DSM2542-DCrib as described previously[19]. To construct the plasmid XW55-P15, the P15 gene fragment was amplified from plasmid pUC19 using the primer pair P15-F/R, and assembled with the plasmid backbone amplified from plasmid XW55[43,44] using the primer pair XW55-P15-GJ-F/R.

To activate the metabolic pathway from xylose to riboflavin using the selected three xylose-inducible promoters P_{11585} (S), P_{16610} (M) and P_{03225} (W), we constructed a series of plasmids named p*i*prs-p*j*purine-p*k*riboflavin (*i*, *j* and *k* indicate one of S, M and W, respectively. Supplementary Table 7) by yeast-based transformation-associated recombination[43,44]. Firstly, we prepared eight linear DNA fragments, consisting of (1) the fragment of 2u-ori origin of replication and URA3 amplified from plasmid XW55-P15 using primer pair JM-F/R, (2) the *repBST1* origin of replication and kanamycin resistance gene from plasmid pUCG18-sfgfp using primer pair ZLGJ-F/R, (3) the *prs* gene amplified from the genome of DSM 2542 using primer pair prs-F/R, (4) the purine gene cluster amplified from the genome of DSM 2542 using primer pair purine-F/R, (5) the *rib* cluster amplified from the genome of DSM 2542 using primer pair Rb-F/R, (6) the promoters S, M and W (amplified from the genome of DSM 2542 using primer pairs S-zl-F/S-pr-R, M-zl-F/M-pr-R and W-zl-F/W-pr-R, respectively) used for linking the DNA fragments generated from (2) and (3), (7) the promoters S, M and W (amplified from the genome of DSM 2542 using primer pairs S-pr-F/S-pu-R, M-pr-F/M-pu-R and W-pr-F/W-pu-R, respectively) used for linking the DNA fragments generated from (3) and (4), (8) the promoters S, M and W (amplified from the genome of DSM 2542 using primer pairs S-pu-F/S-Rb-R, M-pu-F/M-Rb-R, and W-pu-F/W-Rb-R, respectively) used for linking the DNA fragments generated from (4) and (5). Each of the DNA fragments contained a minimum of 35 bp overlapping sequences with the flanking fragments. Then, each combination of the fragments were co-transformed into *S. cerevisiae* BJ5464-NpgA (*MATα ura3-52 his3-Δ200 leu2-Δ1 trp1 pep4::HIS3 prb1Δ1.6R can1 GAL*)[44] using *S. cerevisiae* EasyComp Transformation Kit (Invitrogen). The correct yeast transformants were verified by PCR and DNA sequencing. Next, the plasmids were isolated from the yeast transformants using Zymoprep (D2001) Kit (Zymo Research) and transformed into *E. coli* Top10. The *E. coli* competent cells were produced and transformed according to the transformation and storage solution protocol[62]. Finally, the plasmids were transformed into *G. thermoglucosidasius* as described previously by Cripps[19].

Total RNA isolation. The *G. thermoglucosidasius* DSM 2542 strains cultivated in liquid USYE medium were harvested by fast filtration, flash frozen in liquid nitrogen, and ground into powder for total RNA extraction using TRNzol (Tiangen, China). The integrity and quantity of the isolated RNA were checked by denaturing agarose gel electrophoresis and NanoDrop 2000 spectrophotometer (NanoDrop Technologies, USA), respectively.

RNA-Seq analysis. The cultures of *G. thermoglucosidasius* DSM 2542 in liquid USYE with 1% xylose or without xylose were sampled at 4 h, 6 h and 8 h, and used for massively parallel cDNA sequencing. The cDNA libraries were prepared and analyzed on Illumina HiSeq 2000. Samples were sequenced twice to obtain appropriate deep sequencing results. Raw data were processed by removing those with low quality (phred quality < 5) and sequencing adaptors. The remaining clean reads were aligned to the genome of DSM 2542. Mapping the total number of reads to each gene was implemented by Picard tools (http://picard.sourceforge.net/). The promoter strength could be reflected by RPKM, which was calculated with our previous reported formula[63]. The operons were predicted by DOOR 2.0[64] and Rockhopper[65] based on the RNA-Seq data, and manually confirmed.

GFP fluorescence assay. The *sfGFP*[18] was used as a reporter to characterize the performance of these promoters. The *G. thermoglucosidasius* strains carrying the GFP reporter plasmids were cultured overnight at 60°C in USYE medium with corresponding concentrations of glucose or xylose. Then, 2 μL of these cultures were inoculated into 100 μL of fresh pre-heated media in flat-bottom 96-well microtiter plate (Greiner Bio-One) and sealed airtight with VIEWSeal (In Vitro) to prevent water evaporation. The GFP fluorescence was measured using an ELx808™ Microplate Reader (BioTek) with excitation at 485 nm and emission at 535 nm. Values at the middle of log phase were taken for analysis.

To test the transcription time course of these promoters, fluorescence was measured periodically according to the method described above. To test the dose-dependent activation of these promoters, the GFP fluorescence of cells were measured at different xylose concentrations by flow cytometry (FACS) using a Becton-Dickinson FACSCalibur flow cytometer. For the FACS test, a 100 μL (culture) sample was diluted with PBS to 1 mL, and was analyzed within 10 min with excitation at 488 nm and emission at 580 nm. The cells were assayed at a low flow rate until 20,000 total events were collected. Data were analyzed with the FlowJo FC analysis software 7.6.1.

Analytical Methods. The OD at 600 nm was used to measure cell growth (1 OD_{600} nm = 10^7 cells/mL). The xylose and glucose concentrations were measured by HPLC with an Aminex HPX-87H column (Bio-Rad Laboratories, Hercules, CA) and refractive index detector as descripted previously[21,66]. The concentration of riboflavin was determined by HPLC as descripted previously[67].

Declarations

Data availability

The datasets generated and analyzed during the current study are available from the corresponding author upon request.

Acknowledgements

This work was financially supported by the National Key Research and Development Program of China (No. 2020YFA0907700 and 2020YFA0906800). We thank Prof. Shu-Shan Gao (Institute of Microbiology, Chinese Academy of Sciences) for providing the yeast strains, and Prof. Hairong Cheng (Shanghai Jiao Tong University) for providing the corn cob hydrolysate.

Author contributions

J.W., Z.L., Y.C. and K.F. designed the research. J.W., S.P., and F.Q. performed the experiments. W.W. provided key ideas. Z.L., F.Y., H.W., and Z.X. provided key materials. Z.L. and Y.Y. provided key technological supports. J.W., K.F., G.P. and Y.C. wrote the manuscript.

Competing Interests

The authors declare no competing interests.

References

1. Ko, J. K. & Lee, S.-M. Advances in cellulosic conversion to fuels: engineering yeasts for cellulosic bioethanol and biodiesel production. *Curr. Opin. Biotechnol.* **50**, 72–80 (2018).
2. Bayer, E. a, Lamed, R. & Himmel, M. E. The potential of cellulases and cellulosomes for cellulosic waste management. *Curr. Opin. Biotechnol.* **18**, 237–45 (2007).
3. Gao, M., Ploessl, D. & Shao, Z. Enhancing the co-utilization of biomass-derived mixed sugars by yeasts. *Front. Microbiol.* **9**, 3264 (2018).
4. Kim, J.-H., Block, D. E. & Mills, D. A. Simultaneous consumption of pentose and hexose sugars: an optimal microbial phenotype for efficient fermentation of lignocellulosic biomass. *Appl. Microbiol. Biotechnol.* **88**, 1077–85 (2010).
5. Jeffries, T. W. Emerging technology for fermenting D-xylose. *Trends in Biotechnology* vol. 3 208–212 (1985).
6. Kim, S. R., Ha, S.-J., Wei, N., Oh, E. J. & Jin, Y.-S. Simultaneous co-fermentation of mixed sugars: a promising strategy for producing cellulosic ethanol. *Trends Biotechnol.* **30**, 274–82 (2012).
7. Zhang, G.-C., Liu, J.-J., Kong, I. I., Kwak, S. & Jin, Y.-S. Combining C6 and C5 sugar metabolism for enhancing microbial bioconversion. *Curr. Opin. Chem. Biol.* **29**, 49–57 (2015).
8. Schwechheimer, S. K., Park, E. Y., Revuelta, J. L., Becker, J. & Wittmann, C. Biotechnology of riboflavin. *Appl. Microbiol. Biotechnol.* **100**, 2107–19 (2016).
9. Averianova, L. A., Balabanova, L. A., Son, O. M., Podvolotskaya, A. B. & Tekutyeva, L. A. Production of Vitamin B2 (riboflavin) by microorganisms: An Overview. *Front. Bioeng. Biotechnol.* **8**, 570828 (2020).
10. Liu, S., Hu, W., Wang, Z. & Chen, T. Production of riboflavin and related cofactors by biotechnological processes. *Microb. Cell Fact.* **19**, 31 (2020).
11. Koizumi, S., Yonetani, Y., Maruyama, A. & Teshiba, S. Production of riboflavin by metabolically engineered *Corynebacterium ammoniagenes*. *Appl. Microbiol. Biotechnol.* **53**, 674–9 (2000).
12. Acevedo-Rocha, C. G., Gronenberg, L. S., Mack, M., Commichau, F. M. & Genee, H. J. Microbial cell factories for the sustainable manufacturing of B vitamins. *Curr. Opin. Biotechnol.* **56**, 18–29 (2018).
13. Knorr, B., Schlieker, H., Hohmann, H. P. & Weuster-Botz, D. Scale-down and parallel operation of the riboflavin production process with *Bacillus subtilis*. *Biochem. Eng. J.* **33**, 263–274 (2007).
14. Wu, Q.-L., Chen, T., Gan, Y., Chen, X. & Zhao, X.-M. Optimization of riboflavin production by recombinant *Bacillus subtilis* RH44 using statistical designs. *Appl. Microbiol. Biotechnol.* **76**, 783–94 (2007).
15. Zamboni, N., Mouncey, N., Hohmann, H.-P. & Sauer, U. Reducing maintenance metabolism by metabolic engineering of respiration improves riboflavin production by *Bacillus subtilis*. *Metab. Eng.* **5**, 49–55 (2003).

16. Wang, G. *et al.* Integrated whole-genome and transcriptome sequence analysis reveals the genetic characteristics of a riboflavin-overproducing *Bacillus subtilis*. *Metab. Eng.* **48**, 138–149 (2018).
17. Shi, S., Chen, T., Zhang, Z., Chen, X. & Zhao, X. Transcriptome analysis guided metabolic engineering of *Bacillus subtilis* for riboflavin production. *Metab. Eng.* **11**, 243–52 (2009).
18. Reeve, B., Martinez-Klimova, E., de Jonghe, J., Leak, D. J. & Ellis, T. The *Geobacillus* plasmid set: A modular toolkit for thermophile engineering. *ACS Synth. Biol.* **5**, 1342–1347 (2016).
19. Cripps, R. E. *et al.* Metabolic engineering of *Geobacillus thermoglucosidasius* for high yield ethanol production. *Metab. Eng.* **11**, 398–408 (2009).
20. Lin, P. P. *et al.* Isobutanol production at elevated temperatures in thermophilic *Geobacillus thermoglucosidasius*. *Metab. Eng.* **24**, 1–8 (2014).
21. Yang, Z. *et al.* Engineering thermophilic *Geobacillus thermoglucosidasius* for riboflavin production. *Microb. Biotechnol.* 1751-7915.13543 (2020) doi:10.1111/1751-7915.13543.
22. Zhou, J., Wu, K. & Rao, C. V. Evolutionary engineering of *Geobacillus thermoglucosidasius* for improved ethanol production. *Biotechnol. Bioeng.* **113**, 2156–67 (2016).
23. Kwak, S., Jo, J. H., Yun, E. J., Jin, Y.-S. & Seo, J.-H. Production of biofuels and chemicals from xylose using native and engineered yeast strains. *Biotechnol. Adv.* **37**, 271–283 (2019).
24. Gu, Y. *et al.* Reconstruction of xylose utilization pathway and regulons in Firmicutes. *BMC Genomics* **11**, 255 (2010).
25. Görke, B. & Stülke, J. Carbon catabolite repression in bacteria: many ways to make the most out of nutrients. *Nat. Rev. Microbiol.* **6**, 613–24 (2008).
26. de Assis, L. J. *et al.* The High Osmolarity Glycerol Mitogen-Activated Protein Kinase regulates glucose catabolite repression in filamentous fungi. *PLoS Genet.* **16**, e1008996 (2020).
27. Kim, S.-B., Kwon, D.-H., Park, J.-B. & Ha, S.-J. Alleviation of catabolite repression in *Kluyveromyces marxianus*: the thermotolerant SBK1 mutant simultaneously coferments glucose and xylose. *Biotechnol. Biofuels* **12**, 90 (2019).
28. Bruder, M., Moo-Young, M., Chung, D. A. & Chou, C. P. Elimination of carbon catabolite repression in *Clostridium acetobutylicum*–a journey toward simultaneous use of xylose and glucose. *Appl. Microbiol. Biotechnol.* **99**, 7579–88 (2015).
29. Schmiedel, D., Kintrup, M., Küster, E. & Hillen, W. Regulation of expression, genetic organization and substrate specificity of xylose uptake in *Bacillus megaterium*. *Mol. Microbiol.* **23**, 1053–62 (1997).
30. Luo, Y., Zhang, T. & Wu, H. The transport and mediation mechanisms of the common sugars in *Escherichia coli*. *Biotechnol. Adv.* **32**, 905–19 (2014).
31. Li, R., Chen, Q., Wang, P. G. & Qi, Q. A novel-designed *Escherichia coli* for the production of various polyhydroxyalkanoates from inexpensive substrate mixture. *Appl. Microbiol. Biotechnol.* **75**, 1103–9 (2007).
32. Kim, S. M. *et al.* Simultaneous utilization of glucose and xylose via novel mechanisms in engineered *Escherichia coli*. *Metab. Eng.* **30**, 141–148 (2015).

33. Chen, T., Liu, W. X., Fu, J., Zhang, B. & Tang, Y. J. Engineering *Bacillus subtilis* for acetoin production from glucose and xylose mixtures. *J. Biotechnol.* **168**, 499–505 (2013).
34. Taboada, B., Ciria, R., Martinez-Guerrero, C. E. & Merino, E. ProOpDB: Prokaryotic Operon DataBase. *Nucleic Acids Res.* **40**, D627-31 (2012).
35. Hilden, I., Krath, B. N. & Hove-Jensen, B. Tricistronic operon expression of the genes *gcaD* (tms), which encodes N-acetylglucosamine 1-phosphate uridyltransferase, *prs*, which encodes phosphoribosyl diphosphate synthetase, and *ctc* in vegetative cells of *Bacillus subtilis*. *J. Bacteriol.* **177**, 7280–4 (1995).
36. Zakataeva, N. P. *et al.* Wild-type and feedback-resistant phosphoribosyl pyrophosphate synthetases from *Bacillus amyloliquefaciens*: purification, characterization, and application to increase purine nucleoside production. *Appl. Microbiol. Biotechnol.* **93**, 2023–33 (2012).
37. Lobanov, K. V *et al.* Reconstruction of purine metabolism in *Bacillus subtilis* to obtain the strain producer of AICAR: A new drug with a wide range of therapeutic applications. *Acta Naturae* **3**, 79–89 (2011).
38. Bera, A. K., Zhu, J., Zalkin, H. & Smith, J. L. Functional dissection of the *Bacillus subtilis pur* operator site. *J. Bacteriol.* **185**, 4099–4109 (2003).
39. Shi, S., Shen, Z., Chen, X., Chen, T. & Zhao, X. Increased production of riboflavin by metabolic engineering of the purine pathway in *Bacillus subtilis*. *Biochem. Eng. J.* **46**, 28–33 (2009).
40. Asahara, T. *et al.* Accumulation of gene-targeted *Bacillus subtilis* mutations that enhance fermentative inosine production. *Appl. Microbiol. Biotechnol.* **87**, 2195–207 (2010).
41. Nygaard, P. & Saxild, H. H. The purine efflux pump PbuE in *Bacillus subtilis* modulates expression of the PurR and G-box (XptR) regulons by adjusting the purine base pool size. *J. Bacteriol.* **187**, 791–4 (2005).
42. Pedrolli, D. B. *et al.* A dual control mechanism synchronizes riboflavin and sulphur metabolism in *Bacillus subtilis*. *Proc. Natl. Acad. Sci. U. S. A.* **112**, 14054–9 (2015).
43. Bond, C., Tang, Y. & Li, L. *Saccharomyces cerevisiae* as a tool for mining, studying and engineering fungal polyketide synthases. *Fungal Genet. Biol.* **89**, 52–61 (2016).
44. Yao, Y. *et al.* Catalase involved in oxidative cyclization of the tetracyclic ergoline of fungal ergot alkaloids. *J. Am. Chem. Soc.* **141**, 17517–17521 (2019).
45. Li, H. *et al.* Evaluation of industrial *Saccharomyces cerevisiae* strains as the chassis cell for second-generation bioethanol production. *Microb. Biotechnol.* **8**, 266–74 (2015).
46. Mosier, N. *et al.* Features of promising technologies for pretreatment of lignocellulosic biomass. *Bioresour. Technol.* **96**, 673–86 (2005).
47. Ji, X.-J. *et al.* Elimination of carbon catabolite repression in *Klebsiella oxytoca* for efficient 2,3-butanediol production from glucose-xylose mixtures. *Appl. Microbiol. Biotechnol.* **89**, 1119–25 (2011).

48. Liu, H. *et al.* Co-fermentation of a mixture of glucose and xylose to fumaric acid by *Rhizopus arrhizus* RH 7-13-9. *Bioresour. Technol.* **233**, 30–33 (2017).
49. Kadoya, R., Matsumoto, K., Takisawa, K., Ooi, T. & Taguchi, S. Enhanced production of lactate-based polyesters in *Escherichia coli* from a mixture of glucose and xylose by Mlc-mediated catabolite derepression. *J. Biosci. Bioeng.* **125**, 365–370 (2018).
50. Wang, X., Goh, E.-B. & Beller, H. R. Engineering *E. coli* for simultaneous glucose-xylose utilization during methyl ketone production. *Microb. Cell Fact.* **17**, 12 (2018).
51. Cheng, C. *et al.* Association of improved oxidative stress tolerance and alleviation of glucose repression with superior xylose-utilization capability by a natural isolate of *Saccharomyces cerevisiae*. *Biotechnol. Biofuels* **11**, 28 (2018).
52. Dvořák, P. & de Lorenzo, V. Refactoring the upper sugar metabolism of *Pseudomonas putida* for co-utilization of cellobiose, xylose, and glucose. *Metab. Eng.* **48**, 94–108 (2018).
53. Hori, C. *et al.* High-cell density culture of poly(lactate-co-3-hydroxybutyrate)-producing *Escherichia coli* by using glucose/xylose-switching fed-batch jar fermentation. *J. Biosci. Bioeng.* **127**, 721–725 (2019).
54. Phelan, R. M. *et al.* Development of next generation synthetic biology tools for use in *Streptomyces venezuelae*. *ACS Synth. Biol.* **6**, 159–166 (2017).
55. Wang, X., Ning, X., Zhao, Q., Kang, Q. & Bai, L. Improved PKS gene expression with strong endogenous promoter resulted in geldanamycin yield increase. *Biotechnol. J.* **12**, (2017).
56. Yin, S. *et al.* Identification of a cluster-situated activator of oxytetracycline biosynthesis and manipulation of its expression for improved oxytetracycline production in *Streptomyces rimosus*. *Microb. Cell Fact.* **14**, 46 (2015).
57. Sun, Y., Liu, C., Tang, W. & Zhang, D. Manipulation of purine metabolic networks for riboflavin production in *Bacillus subtilis*. *ACS Omega* **5**, 29140–29146 (2020).
58. Boumezbeur, A.-H., Bruer, M., Stoecklin, G. & Mack, M. Rational engineering of transcriptional riboswitches leads to enhanced metabolite levels in *Bacillus subtilis*. *Metab. Eng.* **61**, 58–68 (2020).
59. Liu, D. *et al.* Development and characterization of a CRISPR/Cas9n-based multiplex genome editing system for *Bacillus subtilis*. *Biotechnol. Biofuels* **12**, 197 (2019).
60. Lee, K. K. M., Da Silva, N. A. & Kealey, J. T. Determination of the extent of phosphopantetheinylation of polyketide synthases expressed in *Escherichia coli* and *Saccharomyces cerevisiae*. *Anal. Biochem.* **394**, 75–80 (2009).
61. Gibson, D. G. *et al.* Enzymatic assembly of DNA molecules up to several hundred kilobases. *Nat. Methods* **6**, 343–345 (2009).
62. Chung, C. T., Niemela, S. L. & Miller, R. H. One-step preparation of competent *Escherichia coli*: transformation and storage of bacterial cells in the same solution. *Proc. Natl. Acad. Sci. U. S. A.* **86**, 2172–5 (1989).

63. Li, S. *et al.* Genome-wide identification and evaluation of constitutive promoters in streptomycetes. *Microb. Cell Fact.* **14**, 172 (2015).
64. Mao, X. *et al.* DOOR 2.0: presenting operons and their functions through dynamic and integrated views. *Nucleic Acids Res.* **42**, D654-9 (2014).
65. McClure, R. *et al.* Computational analysis of bacterial RNA-Seq data. *Nucleic Acids Res.* **41**, e140 (2013).
66. Yang, X. *et al.* AcrR and Rex control mannitol and sorbitol utilization through their cross-regulation of aldehyde-alcohol dehydrogenase (AdhE) in *Lactobacillus plantarum*. *Appl. Environ. Microbiol.* **85**, (2019).
67. Wang, J. *et al.* Improvement of stress tolerance and riboflavin production of *Bacillus subtilis* by introduction of heat shock proteins from thermophilic bacillus strains. *Appl. Microbiol. Biotechnol.* **103**, 4455–4465 (2019).

Figures

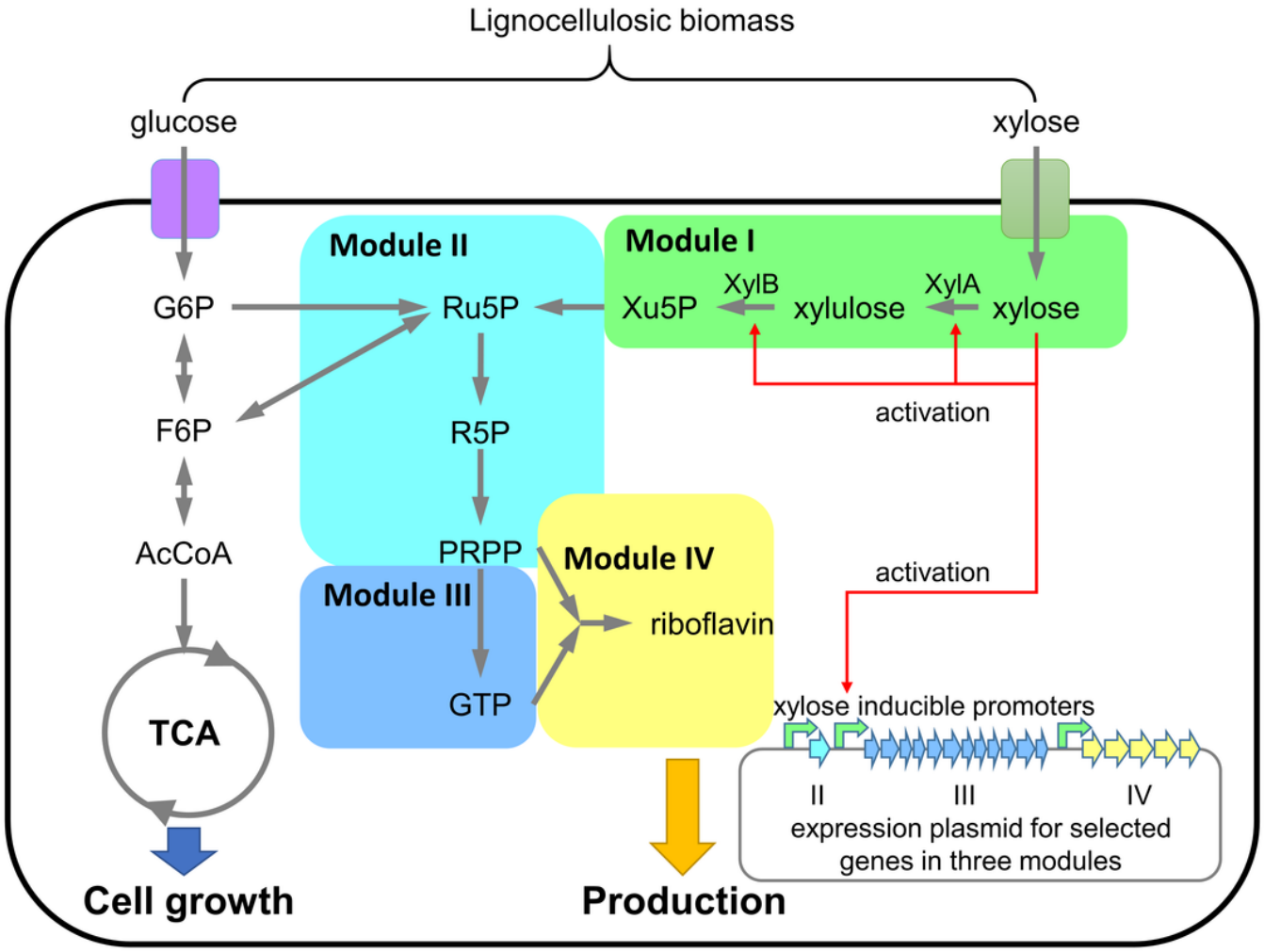

Figure 1

The design of a riboflavin-producing microbial cell factory with the GCR-DC strategy. The biosynthetic process of riboflavin from xylose consisted of four modules. As module I was natively activated by xylose, an extra pathway was constructed on a plasmid to express the engineered modules II–IV that were under the control of xylose-inducible but glucose-insensitive promoters. As a result, the engineered cells would preferentially use glucose for cell growth due to the presence of GCR, and then utilized xylose for the biosynthesis of riboflavin in a later stage.

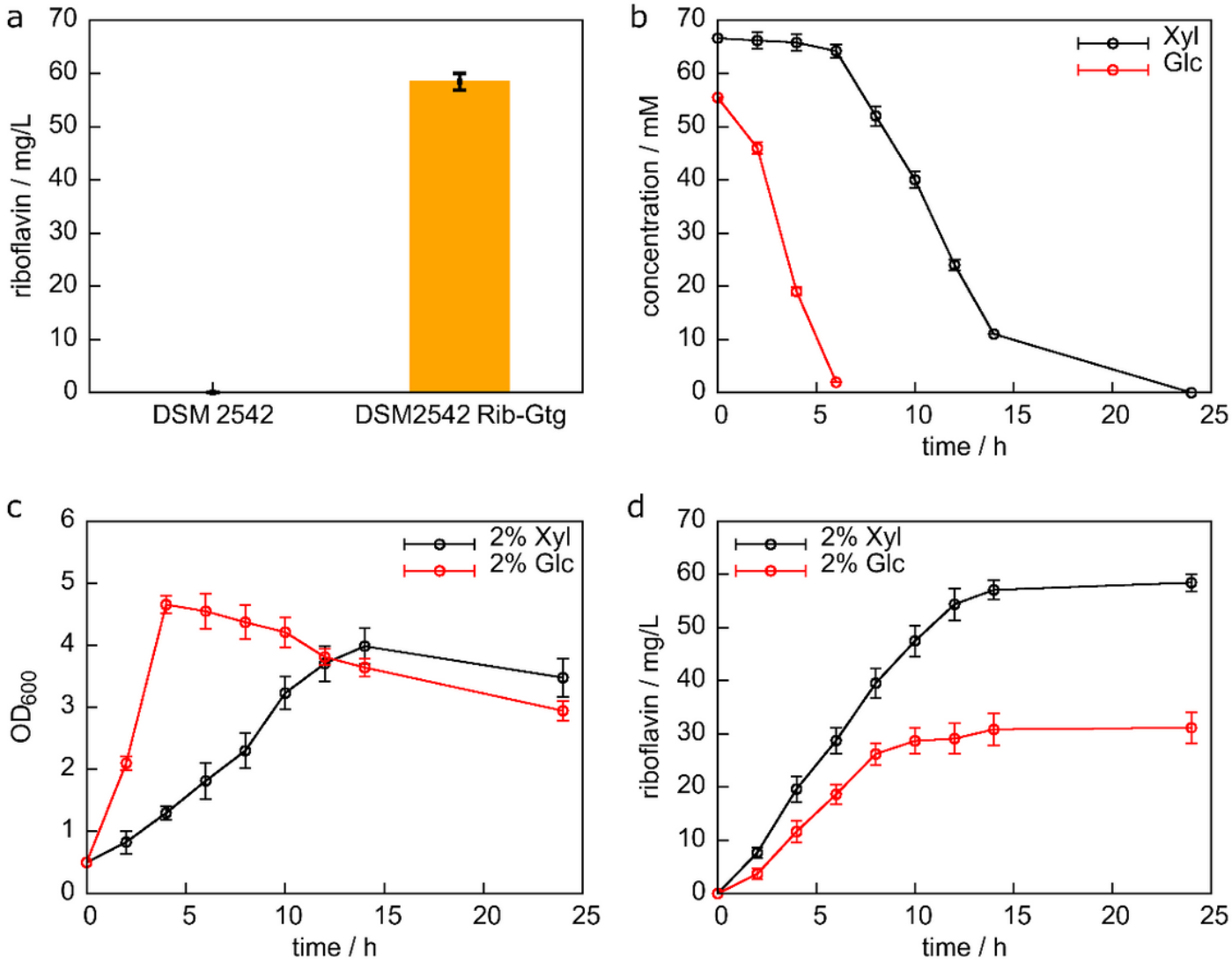

Figure 2

Time profiles of riboflavin production, carbon source consumption and cell growth of DSM2542 Rib-Gtg under different cultivation conditions. a. Riboflavin productions of the strains DSM 2542 and DSM2542 Rib-Gtg in USYE medium supplemented with 2% xylose for 24 h. b. Time profiles of carbon source consumption by DSM2542 Rib-Gtg in USYE medium supplemented with 1% glucose + 1% xylose. c. Growth curves of DSM2542 Rib-Gtg in USYE medium supplemented with 2% glucose or 2% xylose, respectively. d. Time profiles of riboflavin production of DSM2542 Rib-Gtg in USYE medium

supplemented with 2% glucose or 2% xylose, respectively. Xyl, xylose; Glc, glucose. Error bars represented standard deviations of three independent experiments.

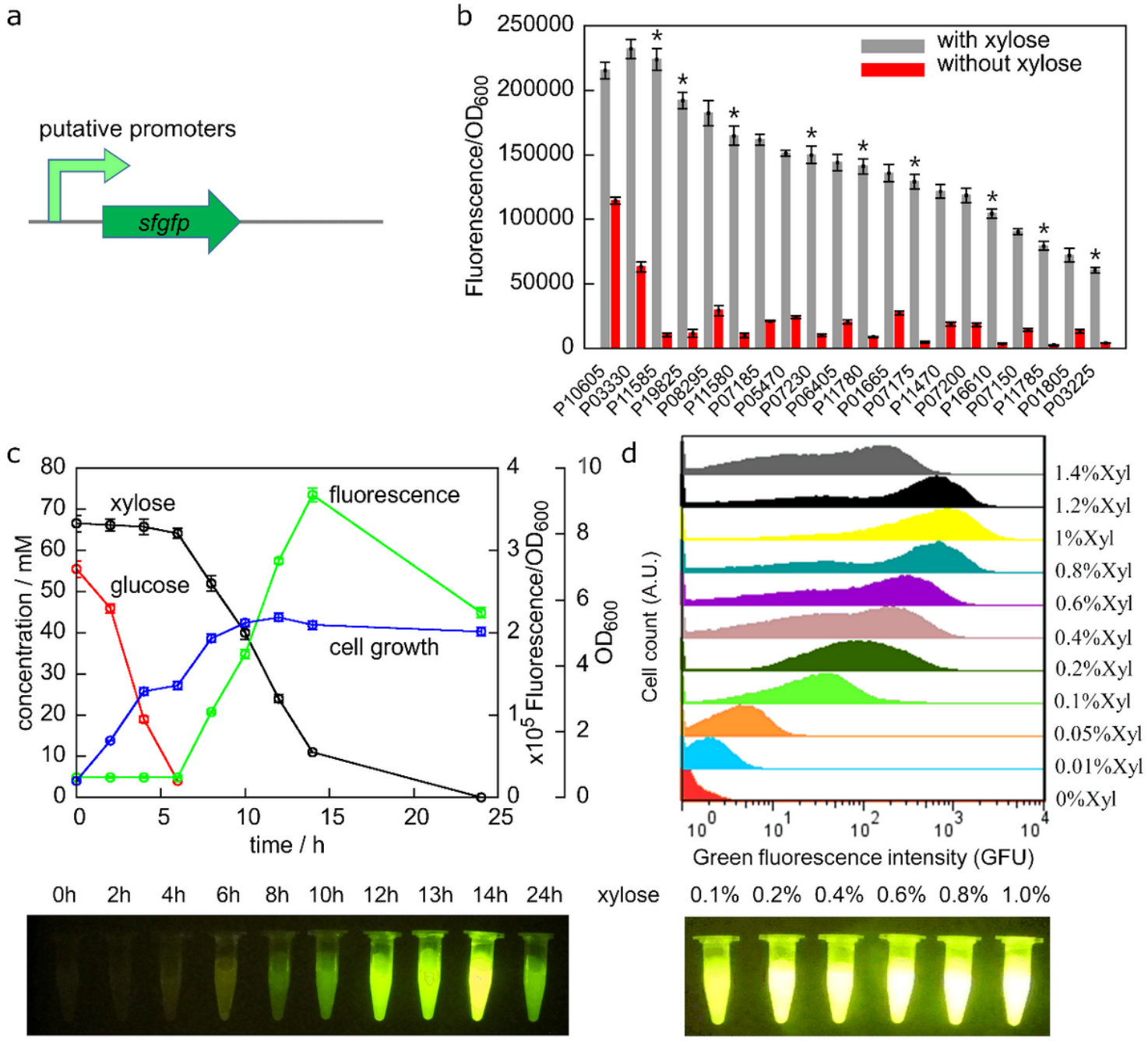

Figure 3

Identification of xylose-inducible and glucose-insensitive promoters. a. A schematic representation of the GFP reporter system. b. Promoter strengths measured by GFP fluorescence. The nine promoters showed little transcription without xylose were labelled by asterisks. Strains were cultured in USYE medium with or without 1% xylose. c. Time courses of glucose consumption (red), xylose consumption (black), cell growth (blue) and GFP fluorescence (green) of the strain DSM2542-RS11585 with the GFP reporter system driven by the promoter P11585. DSM2542-RS11585 was cultured in USYE medium containing 1%

glucose + 1% xylose. d. Dose-dependent activation of the promoter P11585 by different concentrations of xylose using flow cytometer measurements. DSM2542-RS11585 was grown in USYE medium supplemented with a series of different concentrations of xylose as indicated. Error bars represented standard deviations of three independent experiments.

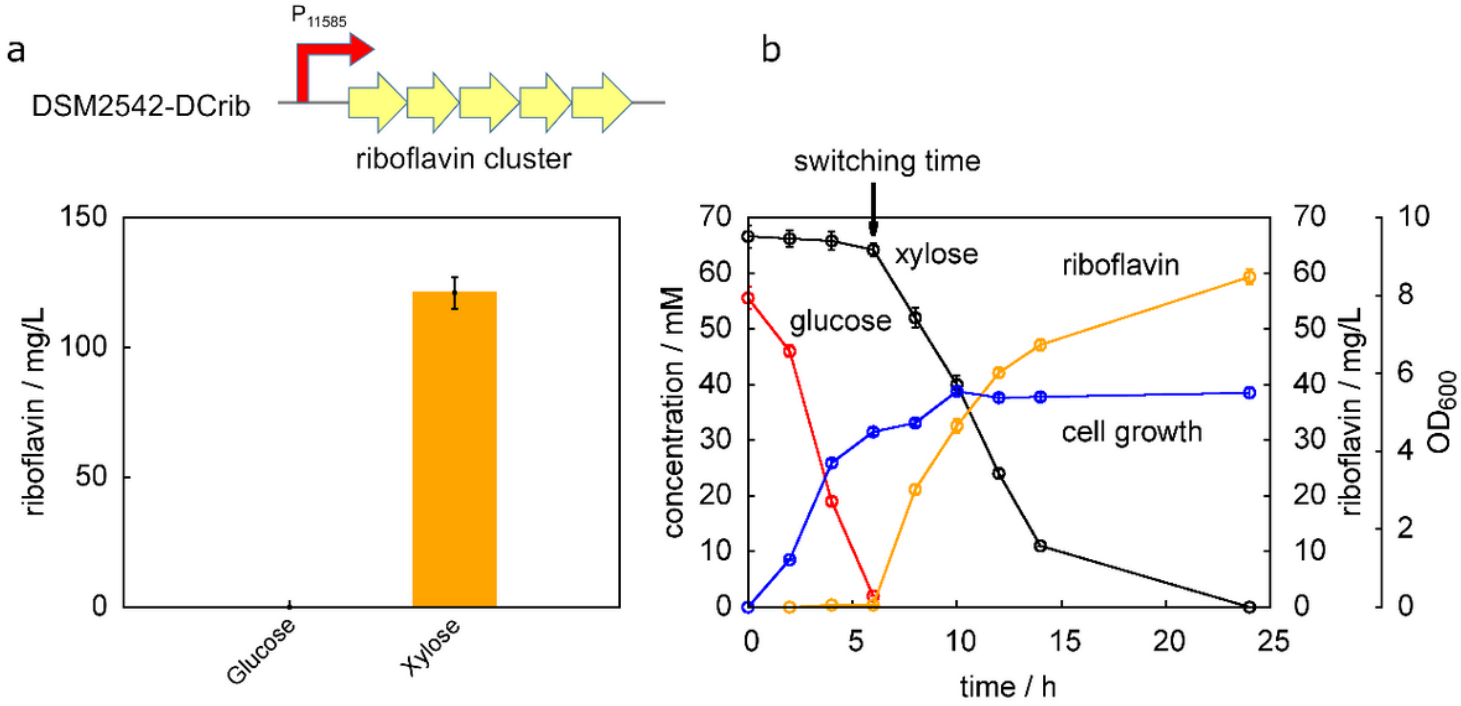

Figure 4

Decoupling the cell growth and riboflavin production in G. thermoglucosidasius DSM2542-DCrib by the GCR-DC strategy. a. Riboflavin production of DSM2542-DCrib in USYE medium with 2% xylose or 2% glucose for 24 h, respectively. b. Riboflavin production (orange), cell growth (OD600, blue) and carbon source utilization (glucose, red; xylose, black) of DSM2542-DCrib cultured in USYE medium with 1% glucose + 1% xylose. Error bars represent standard deviations of three independent experiments.

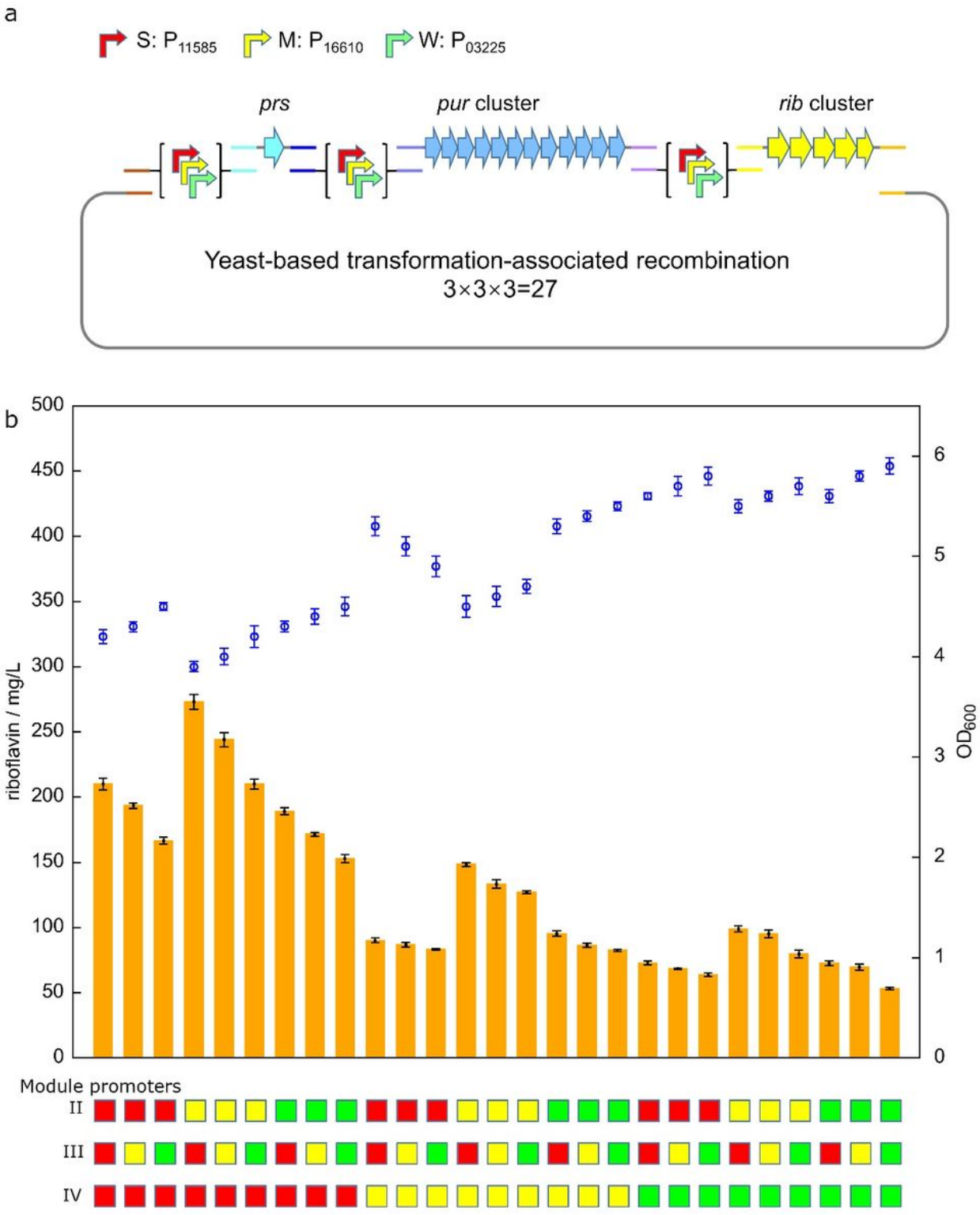

Figure 5

Reconstitution and optimization of the xylose-inducible metabolic pathway from xylose to riboflavin. a. Plasmids harboring the modules II, III and IV controlled by different combinations of promoters. Totally, 27 different plasmids were constructed. The prs gene, 12 genes in pur operon, and the rib cluster were from module II, III, and IV, respectively. b. Riboflavin production (orange bars) and cell growth (OD600, blue symbols) of the 27 engineered strains. S: the strong promoter P11585 (red); M: the medium strength

promoter P16610 (yellow); W: the weak promoter P03225 (green). Error bars represented standard deviations of three independent experiments.

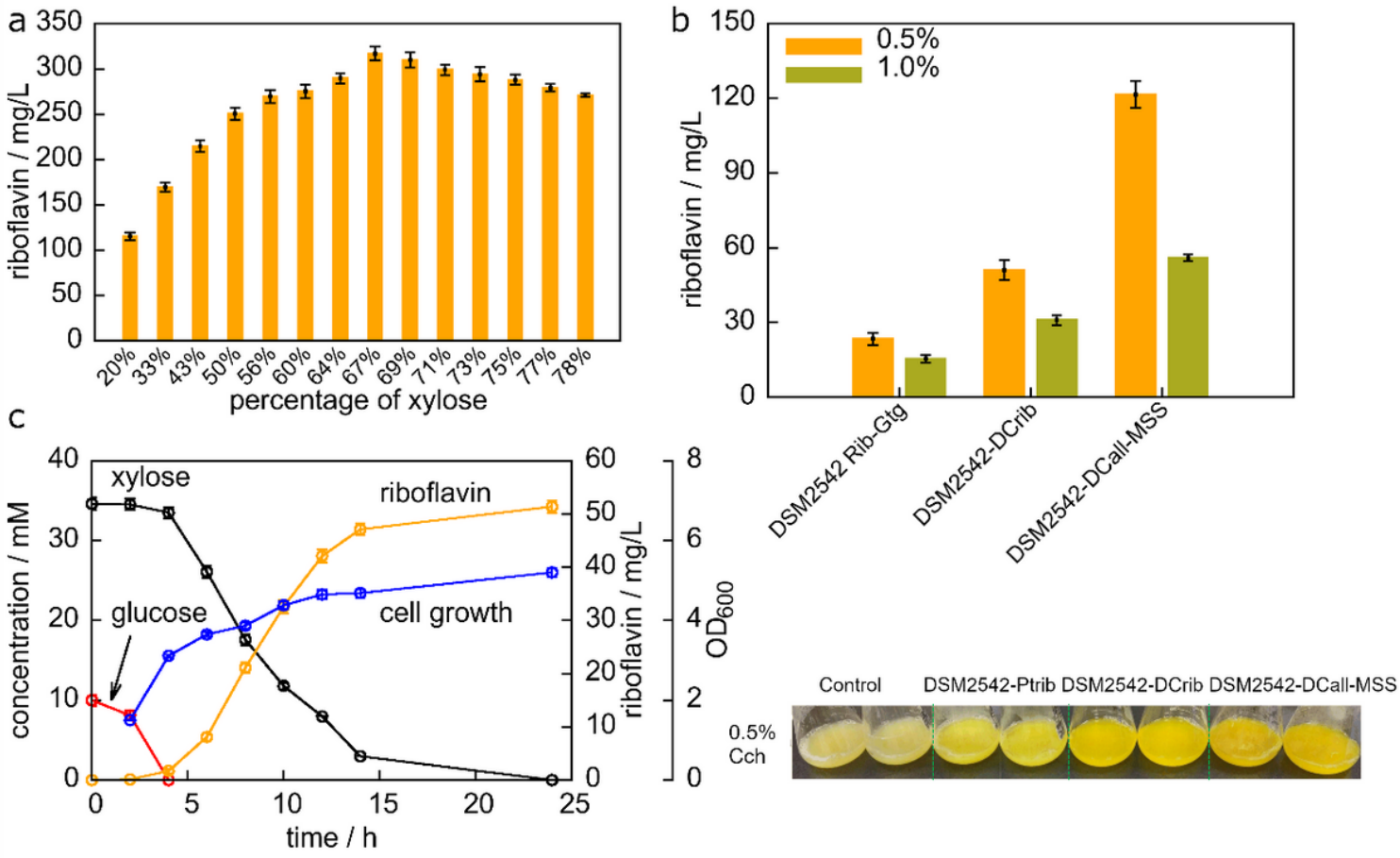

Figure 6

Effects of the xylose/glucose ratios on riboflavin production and the production of riboflavin using the lignocellulosic carbon source. a. Evaluation of the influence of xylose/glucose ratios on the riboflavin production of DSM2542-DCall-MSS. b. Riboflavin productions of DSM2542 Rib-Gtg, DSM2542-DCrib and DSM2542-DCall-MSS using corn cob hydrolysate as a carbon source. Strains were cultivated in USYE medium with 0.5% and 1% corn cob hydrolysates for 24 h, respectively. c. Time courses of glucose concentration (red), xylose concentration (black), biomass (blue), and riboflavin accumulation (orange) of strain DSM2542-DCall-MSS in USYE medium with 1.0% corn cob hydrolysate. Error bars represented standard deviations of three independent experiments.

Supplementary Files

This is a list of supplementary files associated with this preprint. Click to download.

- SI.docx